Tuning the microenvironment of gold nanoparticles encapsulated within MIL-101(Cr) for the selective oxidation of alcohols with O_2. Influence of the amino terephthalate linker.

Andrea Santiago-Portillo,[1,º] María Cabrero-Antonino,[1,º] Mercedes Álvaro,[1] Sergio Navalón,[1,*] Hermenegildo García[1,2,3,*]

[1] Departamento de Química, Universitat Politècnica de València, C/Camino de Vera, s/n, 46022 Valencia, Spain

[2] Instituto de Tecnología Química CSIC-UPV, Universitat Politècnica de València, Consejo Superior de Investigaciones Científicas, Av. de los Naranjos s/n, 46022 Valencia, Spain

[3] Center of Excellence for Advanced Materials Research, King Abdulaziz University, Jeddah, Saudi Arabia

[º] Both are first authors

Abstract: This manuscript reports a comparative study of the catalytic performance of gold nanoparticles encapsulated within MIL-101(Cr) with or without amino groups in the terephthalate linker. The purpose is to show how the amino groups can influence the microenvironment and catalytic stability of incorporated gold nanoparticles. The first influence of the presence of this substituent is the smaller particle size of Au NPs hosted in MIL-101(Cr)-NH_2 (2.45 ± 0.19 nm) compared to the parent MIL-101(Cr)-H (3.02 ± 0.39 nm). Both materials are highly active to promote the aerobic alcohol oxidation and exhibit a wide substrate scope. While both catalysts can achieve turnover numbers as high as 10^6 for the solvent-free aerobic oxidation of benzyl alcohol, Au@MIL-101(Cr)-NH_2 exhibits higher turnover frequency values (12,000 h^{-1}) than Au@MIL-101(Cr)-H (6,800 h^{-1}). Au@MIL-101(Cr)-NH_2 also exhibits higher catalytic stability, being recyclable by 20 times with coincident temporal conversion profiles, in comparison with some decay observed in the parent Au@MIL-101(Cr)-H. Characterization by transmission electron microscopy of the 20-times used samples shows a very minor particle size increase in the case of Au@MIL-101(Cr)-NH_2 (2.97 ± 0.27 nm) in comparison with the Au@MIL-101(Cr)-H analogue (5.32 ± 0.72 nm). The data presented show the potential of a better control of the microenvironment to improve the performance of encapsulated Au nanoparticles.

Introduction

Oxidation of alcohols to the corresponding carbonyl compounds is one reaction of considerable importance in organic synthesis, as well as, from the industrial point of view.[1]Application of the principles of green chemistry has motivated an intensive research to develop catalysts for alcohol oxidation using molecular oxygen as terminal oxidant.[2-4] Among the various transition metal catalysts that have shown activity for this aerobic oxidation, those based on supported metal nanoparticles (NPs) are among the most efficient and selective ones, exhibiting a large scope under wide range of experimental conditions.[2, 3, 5, 6] In this type of heterogeneous catalysts, one of the most important roles of the support is to stabilize the dimensions of gold NPs minimizing their growth by strong metal support interactions.[2, 7, 8]

Extensive study in the literature has shown that the catalytic activity of metal NPs for this aerobic oxidation decreases at the particle size increases.[2] Considering the nature of the supports that have been used to deposit metal NPs and besides organic polymers, carbon materials[8] and large area metal oxides,[2] the use of porous supports has been gaining increasing attention.[5, 9] In this context, metal-organic frameworks (MOFs) having a large surface area with variable porosity have become among the preferred hosts to incorporate and stabilize noble metal NPs and more specifically gold NPs.[9, 10] Immobilization of occluded metal NPs is believed to arise from geometrical constrains of the lattice confining incorporated Au NPs.[5, 9] In this context, in a closely related study, Li-Tang and co-workers reported that gold NPs prepared by colloidal deposition of preformed NPs stabilized by polyvinylpyrrolidone (PVP) incorporated inside MIL-101(Cr)-H is a highly efficient heterogeneous catalyst to promote the aerobic oxidation of alcohols under base-free conditions.[11] Other preparation procedures including colloidal deposition using glucose as protecting agent, impregnation of MIL-101(Cr)-H with $HAuCl_4$ or deposition-precipitation method were much less convenient to efficiently prepare MIL-101(Cr) occluded gold NPs (Au@MIL-101(Cr)). [11]

Continuing with this line of research in the present work we compare the performance and stability of two isostructural MOF materials namely as Au@MIL-101(Cr)-H and Au@MIL-101(Cr)-NH_2 as catalyst. Herein it has been found that by controlling the microenvironment experienced by Au NPs within the MIL-101(Cr)

host with amino groups it is possible to further increase the turnover frequency to unprecedented values. Furthermore, these amino groups increase remarkably the stability of Au NPs in the pores of MIL-101(Cr) to the point that these Au NPs do not undergoing significant size increase upon extensive reuse (20 consecutive catalytic cycles). These results illustrate the potential of organic linker substitution in MOFs to further increase the metal NPs by adjusting their microenvironment within the MOF cavities.

Results and Discussion

Preparation and characterization of Au containing MOFs

MIL-101(Cr)-H and MIL-101(Cr)-NH_2 were prepared using a Cr(III) salt and terephthalic acid or 2-nitroterephthalic acid, respectively, followed in the case of MIL-101(Cr)-NH_2 by post-synthetic reduction of the NO_2 groups using $SnCl_2$, according to reported procedures.[12, 13] Supporting information provides characterization data (XRD, FT-IR, XPS, isothermal N_2 adsorption and ICP-AES) for the two MOFs used in the present study (Figures S1-S4). As previously reported, XRD patterns of MIL-101(Cr) and MIL-101(Cr)-NH_2 confirm that both materials are isostructural (Figure S1a). FT-IR spectroscopy allows observation of the expected functional groups present in the solids namely carboxylates, aromatic ring and/or amino group in the case of MIL-101(Cr)-NH_2 (Figure S1b). XPS further confirms the composition and oxidation state of the elements present in the MIL-101(Cr)-H (Figure S2) and MIL-101(Cr)-NH_2 (Figure S3). Isothermal N_2 adsorption for MIL-101(Cr)-H allows estimating a BET surface area and pore volume of 2,800 $m^2\ g^{-1}$ and 1.7 $cm^3\ g^{-1}$, respectively (Figure S4a). In agreement with previous studies,[12-14] the presence of amino groups in the MIL-101(Cr)-NH_2 solid decreases of the BET surface area (1,550 $m^2\ g^{-1}$) and pore volume (1.15 $cm^3\ g^{-1}$) respect to the parent material (Figure S4b) due to the space needed to accommodate the organic substituents in the cavities of the MOF. ICP-AES analysis of previously acid-digested MIL-101(Cr)-X (X: H or NH_2) samples confirms the expected chromium content according the theoretical formulae $(Cr_3F(H_2O)_2O(C_8H_4O_4)_3$ and $Cr_3Cl(H_2O)_2O(C_8H_3O_4\text{-}NH_2)_3$. Incorporation of gold NPs on these two MOFs was carried out following the double solvent method (DSM) procedure as previously reported.[15] Chemical analysis of gold for samples previously digested in acid media shows that complete gold incorporation has taken place under DSM conditions. Thus, the resulting two isostructural gold containing-MOFs present coincident gold loading of 0.5 wt%. The presence of Au NPs in both materials MIL-101(Cr) and MIL-101(Cr)-NH_2 was determined by DF-STEM (Figure 1) coupled with EDX detector (Figure S5) that also allowed estimating the Au particle size distribution by measuring the size of more than 300 particles. In particular, Au average particle size and standard deviation values of 2.99 ± 1.64 nm and 2.45±0.95 nm were determined for Au@MIL-101(Cr)-H and Au@MIL-101(Cr)-NH_2, respectively. These values are in the same range, although a little larger, than 2.3 ± 1.1 nm estimated for the Au NPs deposited in the MIL-101(Cr)-H sample prepared by colloidal deposition using PVP as protecting agent previously reported.[11] These values are comparable with the dimensions of the pentagonal and hexagonal cages present in the MIL-101(Cr)-H structure that are 2.9 and 3.4 nm, respectively.[16, 17] The somewhat smaller size of Au NPs incorporated inside MIL-101(Cr)-NH_2 could reflect the smaller cavity dimensions for this MOF due to the presence of NH_2 groups protruding inside the cavity space in comparison to MIL-101(Cr). Figure 1 presents selected DF-STEM images of the gold-containing Au@MIL-101(Cr) and Au@MIL-101(Cr)-NH_2 prepared in this study. In spite of the low Au loading and the small particle size of Au NPs occluded in Au@MIL-101(Cr)-H and Au@MIL-101(Cr)-NH_2, it was possible to detect by XRD the peaks corresponding to metallic Au(0) NPs (Figure 1). In particular, the diffraction peaks corresponding to the 111, 200, 311 planes of fcc Au were detectable in the XRD of gold-containing MOFs (Figure 1).

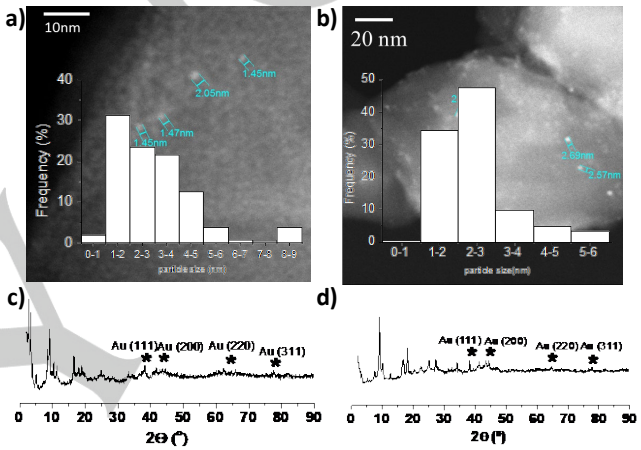

Figure 1. DF-STEM images (a, b), gold particle size distribution inset, and PXRD (c, d) for Au@MIL-101(Cr)-H (a, c) and Au@MIL-101(Cr)-NH_2 (b, d) solids.

The electronic properties of the Au@MIL-101(Cr)-H and Au@MIL-101(Cr)-NH_2 samples were investigated by XPS. XPS spectra shows the expected signals of the elements represent in the samples (Figures S6-S8). Comparison of the XPS Au 4f for Au@MIL-101(Cr)-H and Au@MIL-101(Cr)-NH_2 do not reveal significant differences. Comparison of the XPS N1s for MIL-101(Cr)-NH_2 and Au@MIL-101(Cr)-NH_2 do not reveal significant changes.

Catalytic performance

As indicated in the introduction, the aim of the present study is to determine the influence that the microenvironment caused by amino substituents on the terephthalate linkers plays on the catalytic performance of Au NPs incorporated inside MIL-101(Cr)-H and MIL-101(Cr)-NH_2.

For the initial stage of the study benzyl alcohol was selected as probe molecule to evaluate the catalytic aerobic oxidation. The only product observed in all cases was benzaldehyde. Both Au NPs in MIL-101(Cr)-H and MIL-101(Cr)-NH_2 exhibit very similar catalytic activity under the present reaction conditions, achieving

an almost complete conversion at 50 h reaction time. Figure 2a shows the temporal profiles for benzyl alcohol conversion in the presence of these two catalysts.

Hot filtration test after starting the reaction under the typical reaction conditions and filtering the solid catalyst, while the suspension was hot at 5 h, corresponding to about 25% benzyl alcohol conversion, shows that the reaction stops completely in the absence of solid catalyst (Figure 2a). This observation indicates that the aerobic oxidation is truly heterogeneous and there are not contributions from any soluble species that could have leached from the solid to the liquid phase during the reaction.

The influence of the oxygen pressure on the aerobic benzyl alcohol oxidation was determined by performing benzyl alcohol oxidation at three different oxygen pressures (Figure 2b). A linear relationship between the initial reaction rate and oxygen pressure was determined, indicating that aerobic oxidation follows a first-order kinetics respect to oxygen pressure.

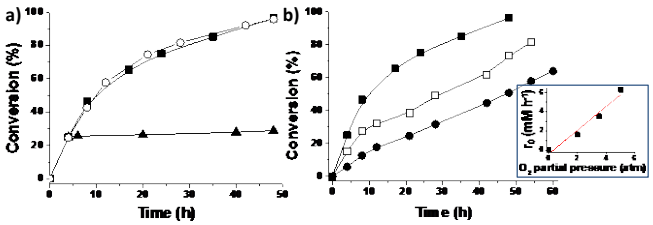

Figure 2. a) Aerobic oxidation of benzyl alcohol using Au/MIL-101(Cr)-H (■) or Au/MIL-101(Cr)-NH_2 (○). Hot filtration test for the MIL-101(Cr)-H catalyst (▲). B) Influence of the oxygen partial pressure for the aerobic oxidation of benzyl alcohol using Au/MIL-101(Cr)-H as catalyst. The inset shows a plot of the initial reaction rate versus O_2 partial pressure.

The nature of the reaction intermediates involved in the process has been addressed by starting the aerobic oxidation of benzyl alcohol under conventional, conditions and adding 20 mol% of different quenchers after 5 h reaction time corresponding to 25 % benzyl alcohol conversion, and monitoring the time-conversion plot after the addition (Figure 3a). It was observed that the presence of *p*-benzoquinone a typical superoxide, hydroperoxyl quencher stops completely the aerobic oxidation, supporting that the evolved of $O_2^{\cdot-}$ is the primary reactive oxygen species generated in the reaction and responsible for the oxidation.[18] Analogously addition of 2,2,6,6-tetramethyl-1-piperidinyloxy (TEMPO) suppresses almost completely the aerobic oxidation, the finally conversion of 50 h being 30 % in comparison to the 25% conversion of benzyl alcohol at the time of TEMPO addition. This result indicates that carbon centered radicals are the intermediates in the process.[13, 18] The small progress from 25 to 30 % observed in benzyl alcohol conversion would indicate an incomplete quenching of these benzylic radicals, probably due to the large molecular size of TEMPO that could not completely trap all the radicals inside the MOF pores. More surprisingly was, however, the notable quenching effect of dimethylsulfoxide (DMSO) and isopropanol in the oxidation. DMSO and isopropanol are selective quenchers of hydroxyl radicals and, therefore, the influence of these compounds suggests that hydroxyl radicals should be somehow generated from superoxide and are responsible for a significant percentage of benzyl alcohol oxidation that can be estimated in about 70 % of the benzyl alcohol converted.[13, 18, 19]

Although quenching by TEMPO is a convincing evidence for the radical nature of the reaction intermediates, transition states leading to these benzylic radicals can have some polar, positive or negative, character due to the asynchronous C-H bond breaking in the parent benzyl alcohol.[11] The polar character of the transition state was investigated by performing under the same reaction conditions the aerobic oxidation of benzyl alcohols having electron donor (i.e. CH_3-) or electron withdrawing (i.e. -NO_2) substituents on the aromatic ring and determining the influence of these groups on the catalytic activity. The temporal profiles of the aerobic oxidation of these benzyl alcohols are shown in Figure 3b. It can be seen there that the presence of NO_2 increases, while the CH_3 group decreases, the initial reaction rate. This influence suggests that the transition state leading to the corresponding benzaldehyde has some anionic character and, therefore, it becomes stabilized by the presence electron withdrawing or destabilized by the presence electron donating groups.

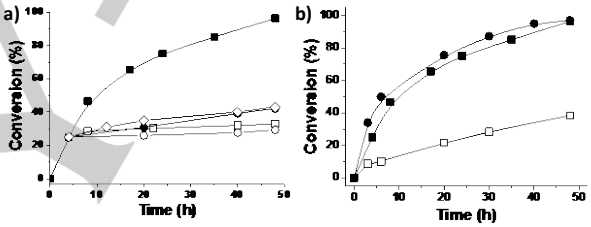

Figure 3. a) Aerobic oxidation of benzyl alcohol in the absence or in the presence of DMSO (●), isopropanol (◊), *p*-benzoquinone (○) or TEMPO (□). b) Comparison of the catalytic activity for the aerobic oxidation of benzyl alcohol (■), 4-nitrobenzyl alcohol (•) or 4-methylbenzyl alcohol (▫) using Au/MIL-101(Cr)-H as catalyst.

The precedent of Au NPs encapsulated within MIL-101(Cr) solid reported in the literature reached a TON and TOF values of about 100 and 250 h^{-1}, respectively, for most of the tested alcohol.[11] The catalyst in that study was reused in the oxidation of the methoxy benzyl alcohol for 6 times without observing deactivation.[11] Herein, we have found that Au@MIL-101(Cr)-H catalyst is able to promote the selective aerobic oxidation of variety of alcohols (1-phenylethanol, 2-hydroxybenzylalcohol, 1-octanol, 2-octanol, cyclohexanol, cinnamyl alcohol and geraniol) to their corresponding carbonyl compounds achieving in all cases a TON value as high as 4,000 and TOF rates ranging from 86 to 606 h^{-1} (Figures S9). To establish further the activity of the present Au@MIL-101(Cr)-H and Au@MIL-101(Cr)-NH_2 a solvent-free productivity test was performed in which a minimal amount of catalyst (1 mg) was used to promote the oxidation of a large excess of benzyl alcohol (25 mmoles). The temporal profiles of this productivity test in the presence of the two Au-containing MIL-101(Cr)-X (X: H or NH_2) catalyst are presented in the supporting information (Figure S10). Under these extreme reaction conditions (substrate to catalyst molar ratio 106) for both MIL-101(Cr)-H and MIL-101(Cr)-NH_2 complete benzyl alcohol conversions at long reaction times (225 h) were achieved

resulting in a TON values as high as 10^6. Notably, higher TOF rates of 12,000 versus 6,800 h^{-1} TOF values were measured under these productivity conditions for Au@MIL-101(Cr)-NH_2 respect to Au@ MIL-101(Cr) at about 10 % conversion. The remarkably higher TOF value measured for Au@MIL-101(Cr)-NH_2 vs Au@MIL-101(Cr)-H shows the benefits on having amino groups interacting with occluded Au NPs. It is remarkable to note that these TON and TOF values are among the highest values reported until now for aerobic alcohol oxidation using heterogeneous catalysts and even much higher than the most active homogeneous catalysis that measured TON and TOF values around ~$1 \cdot 10^5$ and ~$1 \cdot 10^3$ h^{-1}, respectively.[2, 9, 20]

Further evidence to support the positive effect of NH_2 groups on the catalytic performance of encapsulated Au NPs was obtained by performing a series of reusability tests. As it seen can be seen in Figure 4a, upon extensive reuse of Au@MIL-101(Cr)-H some decrease in its catalytic activity was observed by considering the time-conversion plots. This decrease of activity can be clearly observed, for instance, in the 14 and 20 uses. Analysis of the liquid phase in the first use in the case of Au@MIL-101(Cr)-H shows the leaching of only 0.45 wt% of the initial total gold content present in the catalyst to the solution. The extent of gold leaching even further decreases in the subsequent reuses, measuring in the supernatant of the liquid after 4, 14 and 20 uses, values of 0.02, 0.08 and 0.03 wt% of the initial gold content in the catalyst, respectively. TEM images of the used Au@MIL-101(Cr)-H clearly show a gradual growth of the Au particle size from the initial value of the fresh sample (3.02±0.39 nm) to 5.32±0.72 nm for the 20 times used sample (Figure 5a and Table 1). Interestingly, the size increase of Au NPs in the Au@MIL-101(Cr)-H sample upon extensive reuse as catalyst is also reflected in the PXRD patterns of the samples, where the diffraction peaks corresponding to the Au NPs become more intense (Figure 5c).

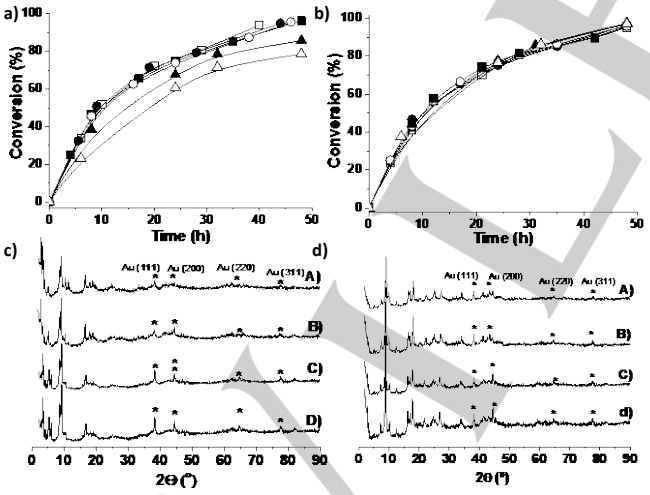

Figure 4. Reusability experiments for the selective aerobic oxidation of benzyl alcohol to benzaldehyde using Au@MIL-101(Cr)-H (a) or Au@MIL-101(Cr)-NH_2 (b) solids as catalysts. Panels c and d show the PXRD of Au@MIL-101(Cr)-H (c) or Au@MIL-101(Cr)-NH_2 (d) before (A) and after the 4th (B), 14th (C) or 20th (D) consecutive uses.

An important observation is that the presence of amino groups in the analogous Au@MIL-101(Cr)-NH_2 catalyst increases the stability of Au NPs. Figure 5b shows the time conversion plot for consecutive reuses up to 20 runs using Au@MIL-101(Cr)-NH_2 as catalyst and observing a remarkable coincidence of the temporal profiles with just very minor catalytic activity decrease. Also, chemical analysis of gold in the supernatant determines lower percentage of Au with values that were 0.48, 0.04, 0.06 and 0.03 wt% of the Au content of the fresh catalyst for the 4, 7, 14 and 20 use of the material, respectively. Importantly, the particle size distribution of Au NPs supported on fresh Au@MIL-101(Cr)-NH_2 (2.45 ± 0.19 nm) only increases slightly after 20 uses (2.97 ± 0.27 nm) (Table 1). In good agreement with this observation of a high stability of Au NPs within MIL-101(Cr)-NH_2, the PXRD of the fresh and used Au@MIL-101(Cr)-NH_2 reveal that the intensity of the Au diffraction peaks are almost unaltered (Figure 5d).

In addition with the high stability catalyst due to the influence of amino groups on the terephthalate linker, one test with 40 mol% of benzoic acid added at initial reaction times shows that this aromatic carboxylic acid does not decrease the catalytic activity of Au@MIL-101(Cr)-NH_2, even in spite of the large percentage respect to the substrate. In previous reports in the literature, it was shown that carboxylic acids, formed as by products due to the over oxidation of aldehydes, can act as poisons in the aerobic oxidation by interacting strongly with the exchangeable coordinated positions of the metal nodes of the MOF that are the active catalytic centers.[9] This situation, however, does not seem to apply in the present case.

Overall this stability study shows that amino groups present in the terephthalate organic ligand of MIL-101(Cr)-NH_2 solid improves catalyst activity and stability, making the growth of Au particle size slower, determining lower Au leaching and making the temporal profile of the oxidation constant for a larger number of reuses.

Figure 5. DF-STEM images and gold particle size distribution of used Au@MIL-101(Cr)-H (a-d) and Au@MIL-101(Cr)-NH_2 (e-h) solids as catalysts for the aerobic oxidation of benzyl alcohol. Legend: 4 uses (a, e), 7 uses (b, f), 14th uses (c, g) and 20th uses (d, h).

Table 1. Summary of the Au average particle size and standard deviation of the fresh and used Au@MIL-101(Cr)-H and Au@MIL-101(Cr)-NH_2 as catalysts during the aerobic oxidation of benzyl alcohol

Catalytic cycles	Au@MIL-101(Cr)	Au@MIL-101(Cr)-NH_2
0 – Fresh sample	3.02 ± 0.39	2.45 ± 0.19
4th	3.12 ± 0.51	2.82 ± 0.36
7th	4.04 ± 0.42	2.89 ± 0.29
14th	5.00 ± 0.70	2.95 ± 0.29
20th	5.32 ± 0.72	2.97 ± 0.27

Conclusions

The importance of the nature of the support is well-stablished in gold catalysis. In this regard, immobilization of Au NPs inside porous hosts has been shown to be a general methodology to increase catalyst stability by impeding the tendency of Au NPs to grow in size. The case of Au NPs inside MOFs being proposed as a clear example of this strategy. Going further, the present study has shown that tuning of the MOF microenvironment by introducing in the organic linker groups that can interact with the Au NPs, stabilizing them, makes possible to increase further the catalytic activity and stability of the incorporated Au NPs. In this way, Au@MIL-101(Cr)-NH_2 appears an among the most efficient catalyst for aerobic oxidation, being stable for a large number of cycles and exhibiting a higher TON than the parent Au@MIL-101(Cr)-H.

Experimental Section

Materials

All the reagents employed in this work were of analytical or HPLC grade and supplied by Sigma-Aldrich.

Catalyst preparation

MIL-101(Cr)-H was prepared and characterized as previously reported.[12, 13, 17] Briefly, a mixture of terephthalic acid (0.25 g, 1.5 mmol), $Cr(NO_3)_3{\cdot}9H_2O$ (0.4 g, 1 mmol) and HF (10 µl) in water (8 mL) was placed in a Teflon-lined autoclave and heated at 200 °C for 8 h. The resulting precipitate was purified by several washings with DMF at 120 ºC and, then, with ethanol at 80 °C for 12 h.

MIL-101(Cr)-NH_2 material was obtained by post-synthetic modification of preformed MIL-101(Cr)-NO_2 following reported procedures.[12, 13] For this purpose, a mixture of 2-nitroterephthalic acid (0.316 g, 1.5 mmol), $CrCl_3$ (0.4 g, 1 mmol) in water (8 mL) was placed in a Teflon lined autoclave and heated at 180 °C for 120 h. The resulting precipitate was purified by several washings with DMF and ethanol. The obtained MIL-101(Cr)-NO_2 solid (200 mg) was suspended in ethanol (60 mL) in the presence of $SnCl_2$ as reducing agent (1.76 g) and the system heated at 80 ºC for 6 h. Finally, the solid was washed several times using Mili-Q water.

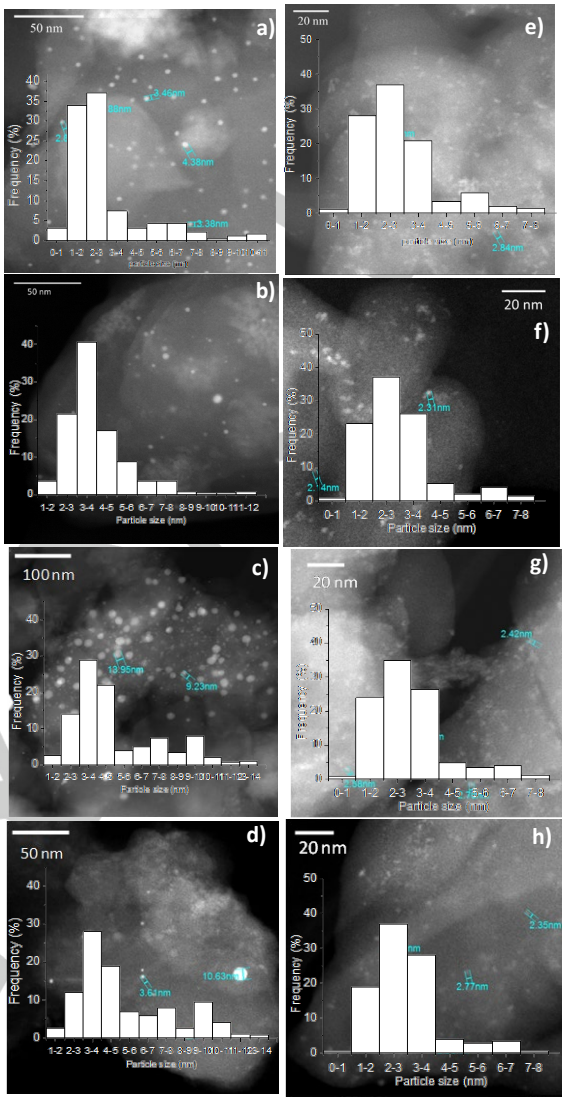

Au NPs were supported in the MIL-101(Cr)-H or MIL-101(Cr)-NH_2 using the previously reported double-solvent method (DSM).[15] In a first step, the MIL-101(Cr)-H and MIL-101(Cr)-NH_2 (200 mg) are thermally activated overnight at 150 ºC under vacuum and, after cooling the system at room temperature, dry n-hexane is added to disperse the solid. To this suspension $HAuCl_4$ dissolved in a minimum amount of water, typically about one-third of the MOF pore volume (360 µL), was suddenly added and the system stirred magnetically for 3 h. After this time the solid was decanted, dried under vacuum and submitted to chemical reduction $NaBH_4$.

Catalyst characterization

Powder X-ray diffractograms (PXRD) were recorded using a Philips X-Pert diffractometer (40 kV and 45 mA) equipped with a graphite monochromator using Ni-filtered CuKα radiation (λ = 1.54056 Å). Attenuated total reflectance Fourier-transform infrared (ATR-FT) spectra were collected using a Bruker Tensor 27 FT-ATR instrument. For these ATR-FT measurements the solid samples were previously dried in an oven for at least 12 h at 100 ºC and, then, equilibrated at room temperature. X-ray photoelectron spectroscopy (XPS) measurements of the solid samples were performed on a SPECS spectrometer equipped with an MCD-9

detector using a monochromatic Al (Kα= 1486.6 eV) X-ray source. Spectra deconvolution was performed using the CASA software after Shirley background correction and setting at 284.4 eV the C1s peak as reference. Isothermal nitrogen adsorption measurements were performed using an ASAP 2010 Micrometrics apparatus. The chromium and/or gold content of the solids were determined by using inductively coupled plasma combined with optical atomic emission spectroscopy detection (ICP-OES). For analysis, the solid sample (20 mg) was previously digested in concentrated HNO_3 solution (20 mL) at 80 ºC for 12 h. Gold leaching was assessed by ICP-OES in the liquid reaction phase after removal the solid catalyst, concentration of the reaction mixture and re-dissolving the residue in Milli-Q water (30 mL). A JEOL JEM-2100F instrument operating at 200 kW under dark-field scanning transmission electron microscopy (DF-STEM) was employed to estimate the Au particle size distribution by measuring more than 300 particles. An EDX detector (Oxford instrument) coupled to the DF-STEM measurements was employed to carry out the microanalysis of the particles present in the solid sample.

Catalytic experiments

Au@MIL-101(Cr)-X (X = H, NH_2) were used as solid catalysts. Briefly, the catalyst (10 mg, 0.00025 mmol of Au) was introduced into a reactor vessel (5 mL) containing the corresponding alcohol (1 mmol) dissolved in toluene (2.5 mL). The system was sonicated (450 W for 20 min) and, then, pressurized with molecular O_2 (5, 3.5 or 2 atm). The reaction system was placed in a preheated oil bath at 160 ºC under magnetic stirring (600 rpm) to ensure that the process is under kinetic control.

For the reusability experiments, the solid catalyst was recovered by filtration (Nylon membrane, 0.2 μm) at the end of the reaction, transferred to a round-bottom flask (50 mL) and washed under magnetic stirring with ethanol (20 mL) at 80 ºC for 2 h. This washing procedure was repeated three times. The resulting solid was recovered by filtration (Nylon membrane, 0.2 μm), dried in an oven at 100 ºC for 24 h and used for a new catalytic cycle.

Selective radical quenching experiments were carried out following the general reaction procedure described above, but with the addition of radical quenchers (20 mol% with respect to the substrate). In particular, DMSO [13, 18, 21], isopropanol,[19] *p*-benzoquinone or TEMPO [13, 18, 22] were used as selective hydroxyl, superoxide/hydroperoxyl and C-centered radical scavengers, respectively.

Poisoning experiments were also carried out following general reaction conditions but with the addition of benzoic acid (20 mol% respect to the substrate).

Productivity tests were carried out under solvent-free conditions using a minimum amount of solid catalyst (1 mg) dispersed in neat benzyl alcohol (25 mmol) working under O_2 atmosphere (5 bar) at 160 ºC.

Product analysis

Previously filtered reaction aliquots were diluted in toluene containing a known amount of nitrobenzene as external standard. The aliquots were analyzed immediately after extraction by gas chromatography using a flame ionization detector. Quantification was carried out based on calibration curves of authentic samples using nitrobenzene as standard. Mass balances for all the reactions were higher than 95 %. Product yields can be estimated by multiplying conversion by selectivity.

Acknowledgements

Financial support by the Spanish Ministry of Economy and Competitiveness (Severo Ochoa, CTQ2015-65963-CQ-R1 and CTQ2014-53292-R) is gratefully acknowledged. Generalidad Valenciana is also thanked for funding (Prometeo 2017/083). S.N. thanks financial support by the Fundación Ramón Areces (XVIII Concurso Nacional para la Adjudicación de Ayudas a la Investigación en Ciencias de la Vida y de la Materia, 2016).

Keywords: heterogeneous catalysis • aerobic oxidation • alcohol oxidation • gold catalysis • MIL-101(Cr)-NH_2

[1] E. Höft, H. Kosslick, R. Fricke, H.-J. Hamann, *Adv. Synth. Catal.* **1996**, *338*, 1-15 ; T. Matsumoto, M. Ueno, N. Wang, S. Kobayashi, *Chem.-Asian J.* **2008**, *3*, 196-214 ; R. A. Sheldon, I. W. C. E. Arenas, *Adv. Synth. Catal.* **2004**, *346*, 1051-1071 ; M. Saikia, D. Bhuyana, L. Saikia, *New J. Chem.* **2015**, *39*, 64-67.

[2] A. Corma, H. Garcia, *Chem. Soc. Rev.* **2008**, *37*, 2096-2126

[3] S. E. Davis, M. S. Ide, R. J. Davis, *Green Chem.* **2013**, *15*, 17-45 ; C. Parmeggiani, F. Cardona, *Green Chem.* **2012**, *14*, 547-564.

[4] T. Punniyamurthy, S. Velusamy, J. Iqbal, *Chem. Rev.* **2005**, *105*, 2329-2363; S. S. Stahl, *Angew. Chem. Int. Ed,* **2004**, *43*, 3400-3420.

[5] A. Dhakshinamoorthy, H. Garcia, *Chem. Soc. Rev.* **2012**, *41*, 5262-5284

[6] M. Alhumaimess, Z. Lin, Q. He, L. Lu, N. Dimitratos, N. F. Dummer, M. Conte, S. H. Taylor, J. K. Bartley, C. J. Kiely, G. J. Hutchings, *Chem. Eur. J.* **2014**, *20*, 1701 - 1710; A. Buonerba, C. Cuomo, S. O. Sánchez, P. Canton, A. Grassi, *Chem. Eur. J.* **2012**, *18*, 709 - 715; V. V. Costa, M. Estrada, Y. Demidova, I. Prosvirin, V. Kriventsov, R. F. Cotta, S. Fuentes, A. Simakov, E. V. Gusevskaya, *J. Catal.* **2012**, *29*, 148-156; W. Zhang, Z. Xiao, J. Wang, W. Fu, R. Tan, D. Yin, *ChemCatChem 2019* **2019**, *11*, 1779-1788.

[7] X. Y. Liu, A. Wang, T. Zhang, C.-Y. Mou, *Nano Today* **2013**, *8*, 403-416.

[8] S. Navalon, A. Dhakshinamoorthy, M. Alvaro, H. Garcia, *Coord. Chem. Rev.* **2016**, *312*, 99-148.

[9] A. Dhakshinamoorthy, A. M. Asiri, H. Garcia, *ACS Catal.* **2017**, *7*, 2896-2919

[10] A. J. Howarth, Y. Liu, P. Li, T. C. Wang, J. T. Hupp, O. K. Farha, *Nat. Rev. Mater* **2016**, *1*, 15018; J. Lee, O. K. Farha, J. Roberts, K. A. Scheidt, S. T. Nguyen, J. T. Hupp, *Chem. Soc. Rev.* **2009**, *38*, 1450-1459 ; K. Leus, P. Concepcion, M. Vandichel, M. Meledina, A. Grirrane, D. Esquivel, S. Turner, D. Poelman, M. Waroquier, V. Van Speybroeck, G. Van Tendeloo, H. García, P. Van Der Voort, *RSC Adv.* **2015**, *5*; M. Saikia, V. Kaichev, L. Saikia, *RSC Adv.* **2016**, *6*, 106856-106865.

[11] H. Liu, Y. Liu, Y. Li, Z. Tang, H. iang, *J. Phys. Chem. C* **2010**, *114*, 13362-13369.

[12] M. Lammert, S. Bernt, F. Vermoortele, D. E. De Vos, N. Stock, *Inorg. Chem.* **2013**, *52*, 8521−8528.

[13] A. Santiago-Portillo, J. F. Blandez, S. Navalón, M. lvaro, H. García, *Catal. Sci. Technol.* **2017**, *7*, 1351-1362.

[14] A. Santiago-Portillo, S. Navalón, P. Concepción , M. Alvaro, H. García, *ChemCatChem* **2017**, *9*, 2506-2511.

[15] A. Aijaz, A. Karkamkar, Y. J. Choi, N. Tsumori, E. Rönnebro, T. Autrey, H. Shioyama, Q. Xu, *J. Am. Chem. Soc.* **201**, *134*, 13926-13929; Q.-L. Zhu, J. Li, Q. Xu, *J. Am. Chem. Soc.* **2013**, *135*, 10210-10213.

[16] Y. F. Chen, R. Babarao, S. I. Sandler, J. W. Jiang, *Langmuir* **2010**, *26*, 8743-8750.

[17] G. Ferey, C. Mellot-Draznieks, C. Serre, F. Millange, J. Dutour, S. Surble, I. Margiolaki, *Science* **2005**, *309*, 2040-2042.

[18] A. Santiago-Portillo, S. Navalon, F. Cirujano, F. Llabrés i Xamena, M. Alvaro, H. Garcia, *ACS Catal.* **2015**, *5*, 3216–3224.

[19] G. V. Buxton, C. L. Greenstock, W. P. Helman, A. B. Ross, *J. Phys. Chem. Ref. Data* **1988**, 513-531; C. L. Clifton, R. E. Huie, *In. J. Chem. Kinet.* **1989**, *8*, 677-687.

[20] A. Dhakshinamoorthy, A. M. Asiriban, H. Garcia, *Chem. Commun.* **2017**, *53*, 10851-10869.

[21] P. Cancino, A. Vega, A. Santiago-Portillo, S. Navalon, M. Alvaro, P. Aguirre, E. Spodine, H. García, *Catal. Sci. Technol.* **2016**, *6*, 3727-3736.

[22] A. Gómez-Paricio, A. Santiago-Portillo, S. Navalón, P. Concepción, M. Alvaro, H. Garcia, *Green Chem.* **2016**, 508-515.

Entry for the Table of Contents

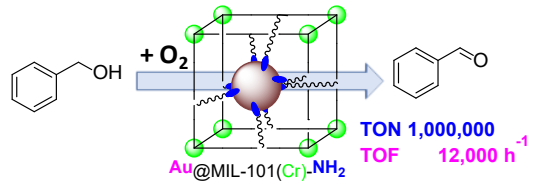

NH_2 groups of terephthalate linkers stabilize encapsulated Au nanoparticles in contact with them, improving further the catalytic activity

Andrea Santiago-Portillo, María Cabrero-Antonino, Mercedes Álvaro, Sergio Navalón, Hermenegildo García**

Page No. – Page No.

Tuning the microenvironment of gold nanoparticles encapsulated within MIL-101(Cr) for the selective oxidation of alcohols with O_2. Influence of the amino terephthalate linker.